# MULTIBIT VERSUS MULTILEVEL EMBEDDING IN HIGH CAPACITY DIFFERENCE EXPANSION REVERSIBLE WATERMARKING

*Dinu Coltuc, Adrian Tudoroiu*

Dept. of Electrical Engineering
Valahia University of Targoviste, Romania
email: {coltuc,tudoroiu}@valahia.ro

## ABSTRACT

The classical difference expansion (DE) reversible watermarking expands two times a difference in order to embed one bit of data. The upper limit of such DE schemes in a single embedding level is usually bounded by 1 bpp. In order to obtain more than 1 bpp, several embedding stages are chained. The multibit DE schemes expand $n$ times the difference in order to embed up to $\log_2 n$ bpp. This paper proposes a multibit extension of the difference expansion reversible watermarking and compares the results with the multilevel embedding case. The multibit reversible watermarking outperforms the multilevel one both in capacity and quality. Experimental results on standard test images are provided.

***Index Terms***— Reversible watermarking, difference expansion, multilevel embedding, multibit embedding

## 1. INTRODUCTION

Difference expansion, introduced by Tian, [1], appears to be the most efficient approach for reversible watermarking. The original approach of Tian considers pairs of disjoint pixels, extends two times the difference between the pixels and embeds one bit of data into the expanded difference. Since at maximum one bit is embedded into each pair of pixels, the maximum capacity provided in a single embedded level by Tian's approach cannot exceed 0.5 bits per pixel.

An increase of the upper bound of the embedding capacity was obtained in [2, 3]. Instead of pairs, they considered groups of $n$ pixels, $n > 2$, and embedded $n - 1$ bits into each group. Compared with Tian's DE, for $n = 3$ and $n = 4$, the upper limit of the embedding capacity increases to 0.67 bpp and $0,75$ bpp, respectively. Even if the theoretical upper limit should increase with $n$, practically the further increase does not provide any gain. By the contrary, the capacity decreases because of the decrease of the number of embedded blocks.

Several improvements of the difference expansion schemes were further provided by Thodi et al., [4]. The difference between adjacent pixels was replaced by the difference between the pixel and its predicted value. In [4], the MED (median edge detector) predictor was used. The prediction error obtained by using MED is lower than the one obtained by using a first order predictor as the adjacent pixel. Lower the prediction error, lower the distortion introduced by the watermarking. In order to reduce the overall error, other predictors or improved embedding schemes have been considered as well (see, for instance, [5]). Furthermore, instead of embedding into pairs of pixels, the embedding is performed into each pixel. In order to recover at detection the same predicted value (i.e., the same prediction context), the embedding and the detection are performed in opposite scan directions. Thus, in [4], the embedding is performed in normal scanning order starting from the upper left corner, while the detection proceeds in reverse order starting from the last embedded pixel. The last row and the last column are not embedded in order to provide the unaltered detection context. The embedding into each pixel provides, in a single embedding level, an upper bound of 1 bpp.

The algorithms discussed above, namely [1, 4, 5], as well as many other versions embed one bit of data by expanding two times a certain difference. By embedding into each pixel, the embedding capacity in a single embedding level is bounded by 1 bpp. By expanding $n$ times the difference, instead of embedding a single data bit, one can embed an integer code in the range $[0, n]$. For $n > 2$, the upper limit of the embedding capacity becomes $\log_2 n$ bpp. Such a multibit embedding scheme was proposed in [6]. The difference between adjacent pixels was expanded $n$ times. The scheme proposed in [6] used an original divisibility based detection scheme that eliminates the need of a location map, but reduces the upper bound to only $\log_2(n-1)$ bpp. Some dependency problems of the scheme of [6] have been reported and corrected in [7]. For classical test images, the version of [7] provides, in a single embedding level, around 1.7 bpp. With a second embedding level, embedding bit-rates of about 2 bpp are obtained.

The results reported so far in the literature for difference expansion watermarking are usually limited to the range (0,1) bpp. The classical two times difference expansion is considered. The embedding capacity is controlled by using a thresh-

This work was supported by UEFISCDI, PN-II-PT-PCCA-2011-3.2-1162 project.

old and by embedding only the pixels where the difference is less than the threshold. For more than 1 bpp embedding capacity, the same schemes are considered in a multilevel embedding context. In order to obtain the needed capacity, after a first embedding stage, a second one is chained and so on.

We strongly consider that the multilevel embedding scenario is less efficient than the multibit one. For instance, let us consider the multilevel prediction error expansion watermarking case. The first embedding stage is performed by increasing two times the prediction error. A second level of embedding demands another increase of two times, i.e., an increasing of four times of the initial prediction errors and so on. One can have pixels where data can be embedded after a three time expansion of the difference, but not after a four times expansion. Therefore, the multibit scenario can provides both higher capacity and lower distortion than the multilevel embedding one. In this context, this paper proposes a multibit extension of the difference expansion reversible watermarking and compares the results with the ones obtained for the multilevel embedding case. The outline of the paper is as follows. The multibit scheme is briefly introduced in Section 2. Experimental results and comparisons with the multilevel embedding are presented in Section 3. Finally, the conclusions are drawn in Section 4.

## 2. MULTIBIT REVERSIBLE WATERMARKING SCHEME

We present the multibit extension of the DE reversible watermarking for the case of a prediction error expansion scheme. Let $x$ be the graylevel of a pixel. If $\hat{x}$ is the predicted value, then the prediction error is:

$$p_e = x - \hat{x} \tag{1}$$

Let further $n$ be a fixed integer, $n \geq 2$ and let $w$ be an integer code in $[0, n-1]$.

### 2.1. Multibit embedding

The data embedding proceeds as follows. The prediction error is expanded $n$ times and the integer code is added to the expanded error:

$$p'_e = np_e + w \tag{2}$$

The embedded new pixel is:

$$x' = \hat{x} + p'_e = x + (n-1)p_e + w \tag{3}$$

The embedded pixel, $x'$, should preserve image gray level range. For 8 bit gray level images, $x' \in [0, 255]$, i.e., $0 \leq x + (n-1)p_e + w \leq 255$. In order to ensure the gray level range regardless $w$, one should have:

$$0 \leq x + (n-1)p_e < 255 - n \tag{4}$$

In fact, only one inequality should be checked. Thus, if $p_e$ is positive one should check only the overflow, otherwise the underflow.

The capacity of the marked image is usually controlled by using a threshold $T > 0$ and by embedding only the pixels where the prediction error is less than the threshold. The control of the embedding capacity limits the distortion introduced by the watermarking. Thus, in order to embed data, together with equation (4), the prediction error should obey:

$$|p_e| < T \tag{5}$$

### 2.2. Multibit decoding

The embedding by equation (3) is invertible. The embedded code can be extracted as:

$$w = (x' - \hat{x}) \bmod n \tag{6}$$

The original pixel is recovered as:

$$x = \frac{x' + (n-1)\hat{x} - w}{n} \tag{7}$$

From equations (7), (6), it immediately appears that the same predicted value $\hat{x}$ should be available at detection. A sufficient condition to recover the original predicted value is to keep unaltered the prediction context.

Let us suppose that the median edge detector (MED) predictor is used as in [4]. MED uses three neighbors $a$, $b$, $c$ to estimate the value of pixel $x$:

$$\hat{x} = \begin{cases} \max(a,b), & \text{if c} \leq \min(a,b) \\ \min(a,b), & \text{if c } \geq \max(a,b) \\ a+b-c, & \text{otherwise} \end{cases} \tag{8}$$

where $a$, $b$, $c$ are the right, lower and lower diagonal neighbors of $x$. If we use the MED predictor, the recovering of $\hat{x}$ needs the original values of the right, lower and lower diagonal neighbors of $x$. For this reason the embedding and the detection are done in opposite scan directions. If the embedding starts from the upper left corner to the right and continues row by row, the detection should start from the lower left corner. Obviously, the last column and the last row of the image should be preserved unaltered. Once the original value of a pixel is recovered, the prediction context to invert the embedding for its left neighbor becomes available and so on.

### 2.3. Modified Histogram Shifting

The recovering process can proceed as soon as the pixels where data have been embedded are known. To locate the embedded pixels two schemes are currently used, location map [1], or histogram shifting (HS) [4]. Since it provides the best results on [0,1], we shall further use the HS approach.

The idea of HS is to translate the graylevel of the pixels that cannot be embedded such that, at detection, their prediction error is greater than the one of the embedded pixels.

At detection, the expanded prediction error of an embedded pixel is $np_e + w$. Since the prediction error before data embedding is bounded by $T$ and $w \in [0, n]$, the upper and lower limits of the prediction error at detection are:

$$-nT < np_e + w < nT + n - 1 \tag{9}$$

Let us consider that pixel $x$ was not embedded because equation (5) is not fulfilled, i.e., $|p_e| \geq T$. In order to be located at detection, the pixel $x$ should be transformed as follows:

$$x_{HS} = \begin{cases} x + (n-1)T, & \text{if } p_e \leq 0, \\ x - (n-1)T + n - 1, & \text{otherwise} \end{cases} \tag{10}$$

Obviously, the prediction error for the transformed pixel is outside the bounds given by equation (9).

### 2.4. Additional information embedding

There are pixels that cannot be shifted because they generate overflow or underflow. For these pixels a binary map is build and lossless compressed. Since the majority of the pixels can be shifted, the overflow/underflow map has a better compression ratio than the simple location map of the not embedded pixels.

The overflow/underflow map should be available at detection together with the parameters of the embedding ($n$, $T$). This information should be embedded as additional information into the watermarked image.

An efficient strategy for additional information embedding is to embed by substitution the additional data ($n$, $T$, the lossless compressed overflow/underflow map, etc.) into the LSBs of the image. The substituted bits should be embedded together with the payload into the image. Thus, the overflow/underflow map is first computed by checking, for each image pixel, if equations (4) and (5) are fulfilled. Once the map is available, the size of the lossless compressed map is determined. The number of pixels whose LSBs should be substituted to hide the map follows by considering the substitution of $b$ bits per pixel, with $b \leq 3$. Let $P$ be the number of pixels to be substituted. The integer $n$, $T$, $b$ and $P$ constitute the header of the marked image. The header needs 28 bits (2 bits for $b$, 4 bits for $n$, 8 bits for $T$ and 14 bits for $P$). The header and the compressed map sequence are concatenated. The marking starts from the upper left corner. Once marked, the $b$ LSBs of the first $P$ pixels are collected and concatenated to the payload in order to be embedded into the image.

At detection, the header is first extracted. Then the bits of the compressed overflow/underflow map are extracted and the map is recovered. The detection starts from the lower right embedded pixel. Pixel by pixel, the embedded data is extracted. By concatenating the original values of the substituted bits to the end of the payload, they are recovered at the beginning of the data extraction procedure. Then, by substituting the original LSBs, the first $P$ marked pixels are restored in order to complete the data extraction and original pixel recovery procedure.

Before going any further a comment should be done. For $n = 2$, the prediction error is expanded two times and 1 bit can be embedded per pixel. The case $n = 2$ and the use of MED predictor corresponds to the classical version of [4], except the improved embedding of the overload data described in 2.4.

**Fig. 1**. Test images: *Lena, Jetplane, Boat* and *Barbara*.

## 3. EXPERIMENTAL RESULTS

The results of the proposed multibit embedding are compared with the ones obtained by multivel embedding of the scheme with $n = 2$. Four graylevel standard test images of sizes $512 \times 512$ are considered. They are: *Lena, Jetplane, Boat* and *Barbara* (Fig. 1).

In order to obtain the results for multilevel embedding, one takes the scheme discussed above for the case $n = 2$. First, the results (PSNR versus capacity) for a single level of embedding are computed. Then, the results for all the combinations of thresholds for two embedding levels are considered. Furthermore, as long as positive capacities are obtained, one collects the results for the three embedding levels, four and, so on. Finally, the best results, PSNR versus capacity, are selected. For the test images considered above, the maximum number of embedding levels is four.

**Table 1**. Maximum embedding capacity [bpp] for multilevel and multibit reversible watermarking.

| Image | Multilevel MED | Multibit MED | Multilevel GAP | Multibit GAP |
|---|---|---|---|---|
| Lena | 2.47 | 2.63 | 2.57 | 2.70 |
| Jetplane | 2.55 | 2.63 | 2.70 | 2.70 |
| Boat | 1.99 | 2.25 | 2.20 | 2.27 |
| Barbara | 1.80 | 1.88 | 1.89 | 1.90 |

The results for multibit embedding are obtained by varying both $n$ and the threshold $T$. The case $n = 2$ corresponds to the scheme used also in multilevel embedding. By increasing $n$, the capacity increases up to a maximum value. The experiments performed so far, shows that, depending on the image at hand, the maximum is obtained for $n \in [8, 16]$. Since further increase of $n$ does not provide any increase of capacity, we take $n \in [2, 16]$ For each $n$, the threshold values are increased as long as positive capacity are obtained. As above, the best results PSNR versus capacity are selected.

The experimental results for multilevel and multibit embedding with MED predictor are plotted in Fig. 2. The solid line represents the results for the multibit embedding, the dashed lines the ones for the multilevel embedding. At low capacity, the results are identical, namely the ones obtained for $n = 2$ in a single embedding level. In order to improve the readability of the plots, we have not displayed the results at low capacity.

As it can be seen in Fig. 2, at medium (around 1 bpp) and high capacity, the multibit embedding introduces lower distortion than the multilevel embedding. The maximum gain is about 6 dB.

The multibit embedding provides also a gain in capacity. The maximum gain appears for the test image *Boat*, namely 0.26 bpp, i.e., $13\%$. The maximum capacity for *Boat*, 2.25 bpp, is obtained for $n = 8$ and $T = 19$. For the test image *Lena*, one gets 2.63 bpp ($n = 12$ and $T = 15$). The gain for *Lena* is about 0.17 bpp, i.e., approximately $7\%$. The maximum capacities for *Jetplane* and *Barbara* are 2.63 bpp ($n = 10$ and $T = 13$) and 1.89 bpp ($n = 10$ and $T = 12$), respectively. The gain for *Jetplane* and *Barbara* is of only 0.08 bpp, approximately $4\%$.

Regarding the embedding capacity, the multibit scheme of Section 2 outperforms the one of [7]. For instance, for the test image *Lena*, in the first level of embedding, the scheme of [7] provides about 1.7 bpp, while the proposed multibit scheme provides 2.63 bpp. The multilevel embedding with the same scheme (with $n = 2$), provides for the same test image 2.47 bpp.

Similar results are obtained if instead of MED one considers the gradient-adjusted predictor (GAP) [8]. Compared with MED, GAP is a more complex predictor. The prediction context is extended from 3 to 7 pixels. While MED detects only the existence of a horizontal/vertical edge, GAP detects also its strength (weak, normal or sharp).

The classical reversible watermarking schemes based on GAP, outperforms the ones based on MED (see [5]). As expected, by replacing MED with GAP, the multibit and the multilevel schemes provide rather similar results (Fig. 3). Finally, the maximum embedding capacity for multilevel and multibit schemes with MED and GAP predictors are presented in Table I.

## 4. CONCLUSIONS

A multibit reversible watermarking embedding scheme has been proposed. Experimental results on some standard test images are provided. As expected, the multibit embedding reversible watermarking outperforms the multilevel one both in quality and embedding capacity. For a single embedding level, the multibit reversible watermarking provides the highest capacity reported so far in the literature.

## 5. REFERENCES


[1] J. Tian, "Reversible Data Embedding Using a Difference Expansion", *IEEE Trans. on Circuits and Systems for Videotechnology*, vol. 13, no. 8, pp. 890–896, 2003.

[2] A. M. Alattar, "Reversible Watermark Using the Difference Expansion of a Generalized Integer Transform", *IEEE Trans. on Image Processing*, vol. 13, pp. 1147–1156, 2004.

[3] D. Coltuc and J-M. Chassery, "Simple Reversible Watermarking Schemes: Further Results", *Electronic Imaging, Visual Communications and Image Processing* SPIE, IS&T, vol. 6072, p. 739-746, 2009.

[4] D. M. Thodi, J. J. Rodriguez, "Expansion Embedding Techniques for Reversible Watermarking", *IEEE Trans. on Image Processing*, vol. 15, pp. 721–729, 2007.

[5] D. Coltuc, "Improved Embedding for Prediction Based Reversible Watermarking", *IEEE Trans. Inf. Forensics Security*, vol. 6, no. 3, 2011.

[6] D. Coltuc, "Improved Capacity Reversible Watermarking", *Proc. ICIP'07*, pp. 249–252, 2007.

[7] M. Chaumont and W. Puech, "A High Capacity Reversible Watermarking Scheme", *Electronic Imaging, Visual Communications and Image Processing* SPIE, IS&T, vol. 7257, 2009.

[8] X. Wu and N. Memon, Context-based, adaptive, lossless image coding, *IEEE Trans. on Communications*, Vol. 45, No. 4, pp. 437 444, 1997.

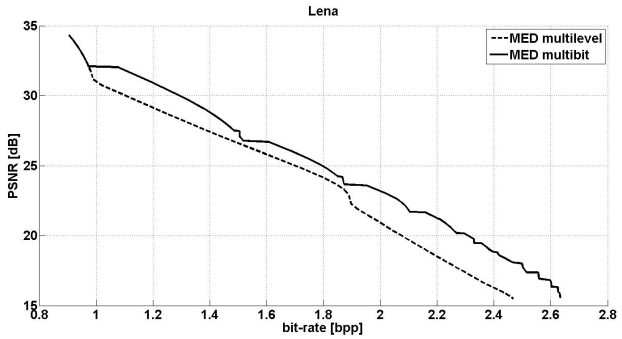


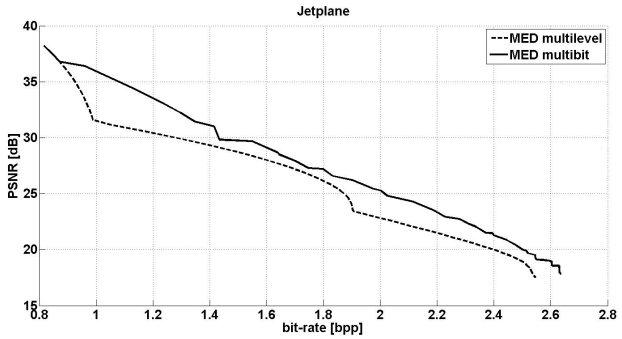


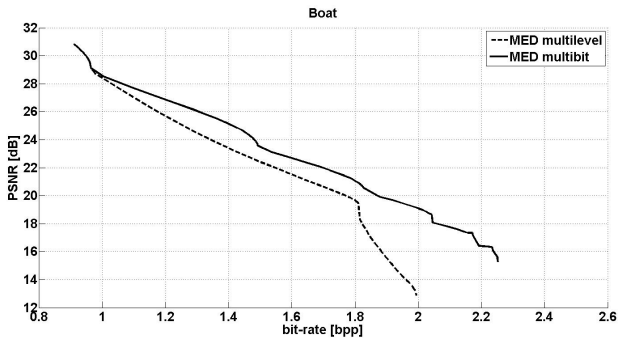


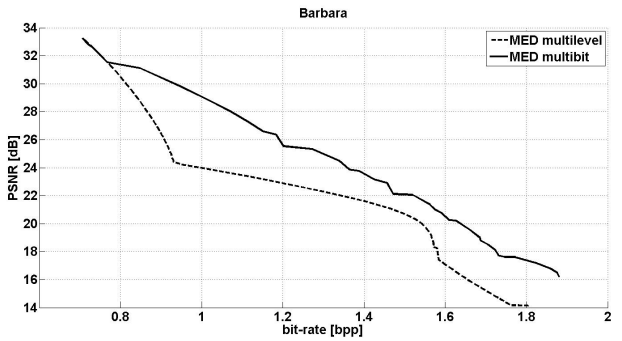


**Fig. 2**. Experimental results for multibit (solid line) and multilevel (dashed line) embedding: MED based scheme.

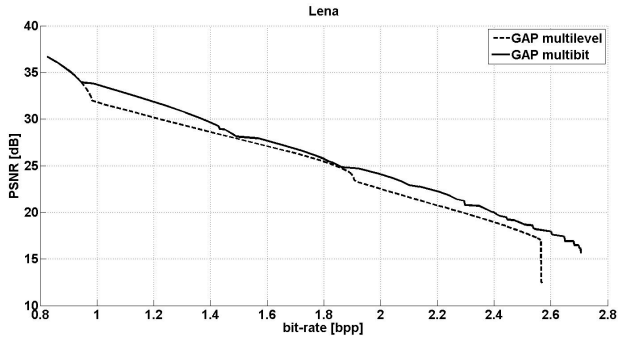


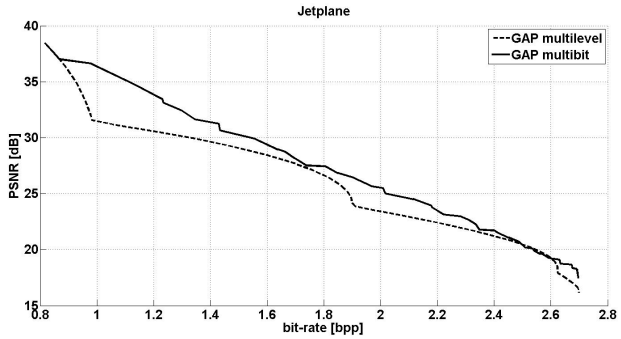


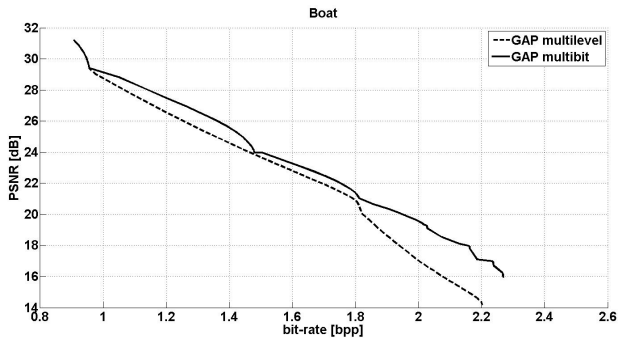


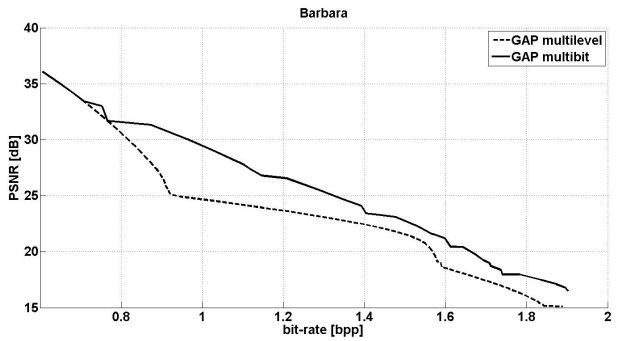


**Fig. 3**. Experimental results for multibit (solid line) and multilevel (dashed line) embedding: GAP based scheme..